Journal of Alloys and Compounds 506 (2010) 963–968

Contents lists available at ScienceDirect

Journal of Alloys and Compounds

journal homepage: www.elsevier.com/locate/jallcom

Structural evolutions of the Fe–40Al–5Cr powders during mechanical alloying and subsequent heat treatment

Haili Liu, Wenming Tang*, Yuexia Wang, Chao Liu, Guangqing Xu, Zhixiang Zheng

School of Materials Science and Engineering, Hefei University of Technology, 193 Tunxi Road, Hefei 230009, Anhui Province, PR China

ARTICLE INFO

Article history:
Received 6 May 2010
Received in revised form 1 July 2010
Accepted 6 July 2010
Available online 24 July 2010

Keywords:
FeAl intermetallic compound
Mechanical alloying
Structural evolution
Ordering transformation

ABSTRACT

Nanocrystalline Fe–40Al–5Cr powders were synthesized by mechanical alloying (MA) of the Fe, Al elemental powders and the Fe–20Cr prealloyed powders. Structural evolutions, morphologies, composition homogenization and ordering transformation of the Fe–40Al–5Cr powders during MA and subsequently heat treatment were studied. In the early stage of MA (<15 h), solid solutions of Fe(Al) and Fe–Cr(Al) form through Al diffusing into Fe and Fe–20Cr, respectively. Layered Fe(Al)/Fe–Cr(Al) laminae are the typical structure of the milled powders. On prolonging the milling time from 15 to 70 h, the layered laminae disappear, and the milled powders turn to be dense, fine and spherical. Meanwhile, the composition homogenization of the milled powders is also gradually accomplished. After the Fe–40Al–5Cr powders milled for 70 h, nanocrystalline Fe(Al, Cr) powders form with a homogeneous composition. During heating the milled powders from room temperature to 600 °C, the ordering transformation from Fe(Al, Cr) to B2-FeAl(Cr) occurs. The Cr content in the Fe–40Al–5Cr powders was found to hinder the composition homogenization and ordering transformation of the powders during MA and subsequent heat treatment.

1. Introduction

FeAl intermetallic compound and its alloys are considered as one kind of the potential structural materials, especially used in aeronautics and astronautics, automobiles, and etc., owing to their excellent oxidation, corrosion and wear resistance, low density, high strength, and so on [1–3]. However, to develop the FeAl structural materials, two major obstacles, i.e. low ductility at ambient temperature and poor strength and creep resistance at 600 °C and above, have been encountered [4]. Previous research has determined that Cr can improve both the ductility of FeAl at room temperature and the strength of FeAl at high temperature. For example, 2–6 at% of Cr in FeAl can significantly enhance the fractural strength and the deformation ability of FeAl by decreasing the anti-phase boundary (APB) energy and the long-range ordering degree and increasing the dislocation motion resistance in FeAl [5,6]. Moreover, Cr in FeAl helps to build a dense oxide film on FeAl, which is believed to increase the toughness of FeAl by inhibiting or even preventing the reaction of Al in FeAl with water vapor in ambient environment [7]. Fe–40Al–5Cr alloy (atomic ratio throughout the context, except where indicated out) is generally taken as the base material to develop many new FeAl alloys and composites [5,8].

Both pure Cr metal and the Fe–Cr prealloy are practically used as Cr source in preparing Cr-containing Fe based alloys. The Fe–Cr prealloy is chosen because it has low Cr loss due to oxidation during high-temperature preparation of Cr-containing Fe based alloys in both casting and powder metallurgy processes. The Fe–Cr prealloy can also make the uniform distribution of Cr in the Fe based alloys easier. As such, the Fe–Cr prealloy is commonly used in preparing the Cr-containing FeAl intermetallic alloy, named FeAl(Cr) in the present paper. Generally, the FeAl(Cr) bulk material is formed by casting process [9], fabrication of FeAl(Cr) via a solid-state process of powder metallurgy has not been reported yet. Therefore, we are interested in fabricating the FeAl(Cr) bulk materials through a powder metallurgy process of hot pressing. In this project, the FeAl(Cr) powders of the Fe–40Al–5Cr composition should be firstly synthesized. In the current study, Fe, Al elemental powders and Fe–20Cr prealloyed powders were employed to synthesize nanocrystalline Fe–40Al–5Cr powders by using the mechanical alloying technique of high-energy ball milling. Structural evolutions, morphologies, composition homogenization and ordering transformation of the powders were studied during mechanical alloying and subsequently heat treatment. Alloying mechanism of the Fe–40Al–5Cr powders during ball milling was also discussed.

2. Materials and methods

Elemental Fe powders and elemental Al powders (both with purity of 99 wt% (weight percentage) and grain sizes of 10 μm) and Fe–20Cr prealloyed powders with

* Corresponding author. Tel.: +86 551 2901373; fax: +86 551 2901362.
E-mail address: wmtang69@126.com (W. Tang).

0925-8388/$ – see front matter © 2010 Elsevier B.V. All rights reserved.
doi:10.1016/j.jallcom.2010.07.130

an average grain size of 198 μm were used to prepare the Fe–40Al–5Cr alloy powders. No process control agent was used in this study to avoid carbon contamination to the alloys. Hardened steel balls of 12 mm diameter were employed. The weight ratio between the ball to powder was maintained at 10:1 throughout the investigation. To minimize oxidation of the powders, the steel vial was first evacuated with a vacuum pump, and then filled with argon (with the purity of 99.99 vol%). This process was repeated for 3 times to minimize the oxygen content in the container. Then the powders were milled using a GN-2 type ball mill operating at 700 rpm. The powders were milled for times range from 5 to 80 h. When the set milling time was used up, the milled powders were taken from the vial to be characterized as well as subsequent heat treatment.

X-ray diffraction (XRD) analyses of the powders milled for 0–80 h were carried out using a D/max-γB type X-ray diffractometer with Cu Kα radiation (λ = 0.154 nm). A H800 type transmission electron microscope (TEM) was employed to reveal morphologies and structural characteristics of the milled powders. Before TEM analyses, the milled powders were first grinded, ultrasonically dispersed in alcohol, and then glued on copper nets. Morphologies and element distributions of Fe, Al and Cr across the cross-sections of the milled Fe–40Al–5Cr powders were detected using a JSM6490 type scanning electron microscope (SEM) equipped with an INCA energy dispersive X-ray detector (EDX). Before the SEM analyses, the milled powders were firstly embedded in epoxy resin. The samples were then grinded and polished, finally etched in a 4 vol% hydrochloric acid aqueous solution with 0.033 g/ml $FeCl_3$. The ordering transformation of the milled powders was tested using a DSC-60 differential thermal scanning calorimeter (DSC) and XRD. The DSC testing of the milled powders was set from room temperature to 600 °C at a heating rate of 10 °C/min. The DSC heating process was repeated again after the first heated powders were cooled to room temperature. The whole DSC heating process was protected by a 99.99 vol% N_2 atmosphere with a flowing rate of 50 ml/min. The heated powders were then detected using XRD to reveal the ordering transformation of the milled powders during the DSC heating process.

3. Results and discussion

3.1. Structural evolutions of the Fe–40Al–5Cr powders during mechanical alloying

Fig. 1a shows XRD patterns of the Fe–40Al–5Cr powders milled for different times. The diffraction peaks around $2\theta = 42–46^\circ$ of Fig. 1a were magnified in order to see more clearly the structural change of the Fe–40Al–5Cr powders during mechanical alloying (Fig. 1b). The XRD pattern of as-mixed Fe–40Al–5Cr powders (0 h) has the diffraction peaks of body centered cubic (bcc) α-Fe and Fe–Cr, and of face centered cubic (fcc) Al (Fig. 1a). Because the atomic radius of Fe and that of Cr are nearly equal to each other (0.124 nm for Fe and 0.125 nm for Cr, respectively), and Fe and Cr are both of a bcc structure, the XRD diffraction peaks of Fe and Fe–20Cr are nearly overlapped (Fig. 1a). However, as shown in Fig. 1b, the diffraction peaks of Fe–20Cr and those of Fe can be actually separated. Because the atomic radius of Cr is slightly bigger than that of Fe, the 2θ angle of $(1\,1\,0)_{Fe–20Cr}$ (44.462°) is less than that of $(1\,1\,0)_{Fe}$ (44.640°), resulting in that the $(1\,1\,0)_{Fe–20Cr}$ diffraction peak is at the left side of the $(1\,1\,0)_{Fe}$ one. Moreover, as shown in Fig. 1a, the XRD diffraction peaks of Al(2 0 0), (2 2 0), (2 2 2), (4 0 0) and (4 2 0) are overlapped with those of Fe and Fe–20Cr(1 1 0), (2 0 0), (2 1 1), (2 2 0) and (5 1 0), respectively. However, those Al diffraction peaks of odd Miller's numbers, i.e. Al(1 1 1), (3 1 1) and (3 3 1), are not overlapped, which can serve as the indicator to show whether the Al diffraction peaks disappear or not during milling. After the Fe–40Al–5Cr powders were milled for 5 h, the diffraction peaks of Al(1 1 1), (3 1 1) and (3 3 1) disappeared, meanwhile, those of Fe and Fe–20Cr were broaden and shift left side more or less. The 2θ angle of the $(1\,1\,0)_{Fe}$ plane shifts left from 44.640° for the 0 h milled powders to 43.943° for the 5 h milled powders, in the same time, the 2θ angle of the $(1\,1\,0)_{Fe–20Cr}$ plane changes from 44.462° to 44.380°. Therefore, the 2θ angle positions of the diffraction peaks of Fe and those of Fe–20Cr exchanged after the powders milled for 5 h. That is, the Fe diffraction peaks are located on the left of the Fe–20Cr ones for the 5 h milled powders.

The left shift of the Fe and Fe–Cr diffraction peaks refers to the formation of the solid solutions of Al in Fe and Fe–Cr, named Fe(Al) and Fe–Cr(Al), respectively, based on the authors' previous work [10]. So, the disappearance of the Al diffraction peaks of the 5 h milled Fe–40Al–5Cr powders mostly results from the dissolution of Al into Fe and Fe–20Cr to form Fe(Al) and Fe–Cr(Al), although any other factors may also cause the disappearance or declination of the diffraction peaks of Al in the early stage of ball milling [11,12]. Note that the left shift of the Fe(Al) diffraction peaks is definitely faster than that of the Fe–Cr(Al) ones, indicating that more Al dissolves into Fe(Al) than into Fe–Cr(Al). According to Heesemann et al.' research [13], the diffusion coefficient of Al in Fe–19.03Cr alloy is less than that in pure Fe, leading to a faster diffusion of Al into Fe than into Fe–Cr, which provides a reasonable explanation to our experimental result mentioned above.

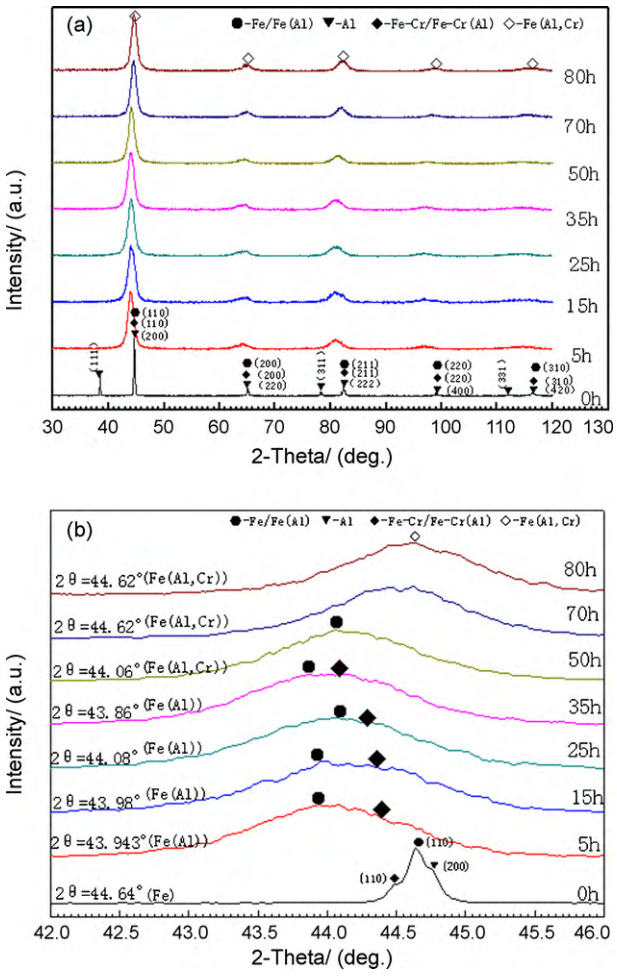

Fig. 1. XRD patterns of Fe–40Al–5Cr powders milled for different times: (a) the whole profile and (b) partial profile magnified for $2\theta = 42–46^\circ$ form (a).

As shown in Fig. 1, the discrepancy of the 2θ angle of the $(1\,1\,0)_{Fe}$ plane and that of the $(1\,1\,0)_{Fe–20Cr}$ plane increases with the milling time. After the Fe–40Al–5Cr powders milled for 35 h, the $(1\,1\,0)_{Fe(Al)}$ diffraction peak shifts left to the largest extent, having a 2θ angle of 43.86° (Fig. 1b). According to the Vegard's rule [11], the Al content in Fe(Al) was calculated to be 22.4 at%, more than the solid solubility of Al in Fe even at 400 °C (20 at%Al, taken from the Fe–Al phase diagram [14]), indicating the formation of a supersaturated solid solution of Fe(Al). In the authors' previous work [10], the Al content in Fe(Al) is as high as 27.4 at% when the Fe–28Al powders were milled for 25 h under the same ball milling condition as the current study. It is 5 at%Al higher than the Al content in Fe(Al) of the Fe–40Al–5Cr powders milled for 35 h. It was concluded that the alloying process of the Fe–40Al–5Cr powders was retarded by introducing the Fe–20Cr prealloyed powders in them. After the

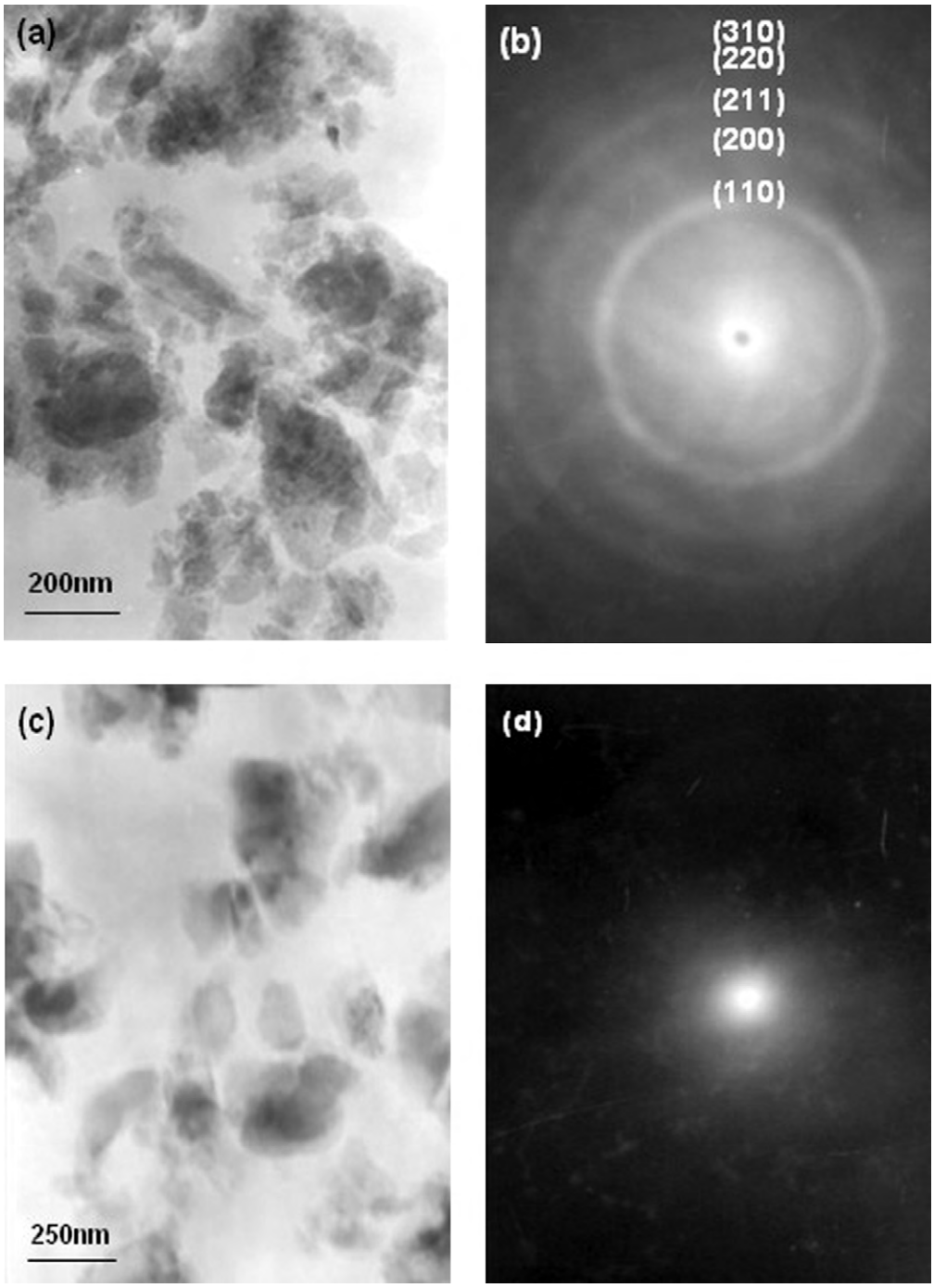

Fig. 2. (a), (c) TEM images and (b), (d) SAED patterns of the Fe–40Al–5Cr powders milled for 35 h and 70 h, respectively.

Fe–40Al–5Cr powders milled for 50 h, the $(1\,1\,0)_{Fe(Al)}$ diffraction peak shifts right, the dissolution of Al from the supersaturated Fe(Al) takes place. On the contrary, the $(1\,1\,0)_{Fe–Cr(Al)}$ diffraction peak keeps shifting left, indicating that the dissolution of Al into Fe–Cr(Al) is still being carried out at that time, which results in the approach of the $(1\,1\,0)_{Fe(Al)}$ and $(1\,1\,0)_{Fe–Cr(Al)}$ diffraction peaks.

In the milled Fe–40Al–5Cr powders, the Al and Cr concentration gradients exist between the Al-rich Fe(Al) and Cr-rich Fe–Cr(Al), They provide a thermodynamic driving force for the mutual diffusion between Al in Fe(Al) and Cr in Fe–Cr(Al). Eventually, the Fe(Al) and Fe–Cr(Al) solid solutions are replaced by a homogeneous solid solution of Al and Cr in Fe, named Fe(Al, Cr). After the Fe–40Al–5Cr powders milled for 70 h, only $(1\,1\,0)_{Fe(Al,Cr)}$ diffraction peak was detected in Fig. 1b, with a 2θ angle of 44.06°. On prolonging the milling time to 80 h, the $(1\,1\,0)_{Fe(Al,Cr)}$ diffraction peak angle does not have any change, showing that the alloying process has finished after the Fe–40Al–5Cr powders milled for 70 h. By using William–Hall formula [15], the average grain size and lattice strain of Fe(Al, Cr) of the 70 h milled Fe–40Al–5Cr powders were calculated to be about 12.9 nm and 0.3%, respectively, according to the XRD result in Fig. 1a.

As shown in Fig. 2, the 35 h milled Fe–40Al–5Cr powders are composed of submicron agglomerates with an average particle size of 250 nm (Fig. 2a). Selected area electron diffraction pattern (SAED) of the powders is of multi rings (Fig. 2b). These diffraction rings are corresponding to the (1 1 0) to (3 1 0) planes of the Fe(Al)

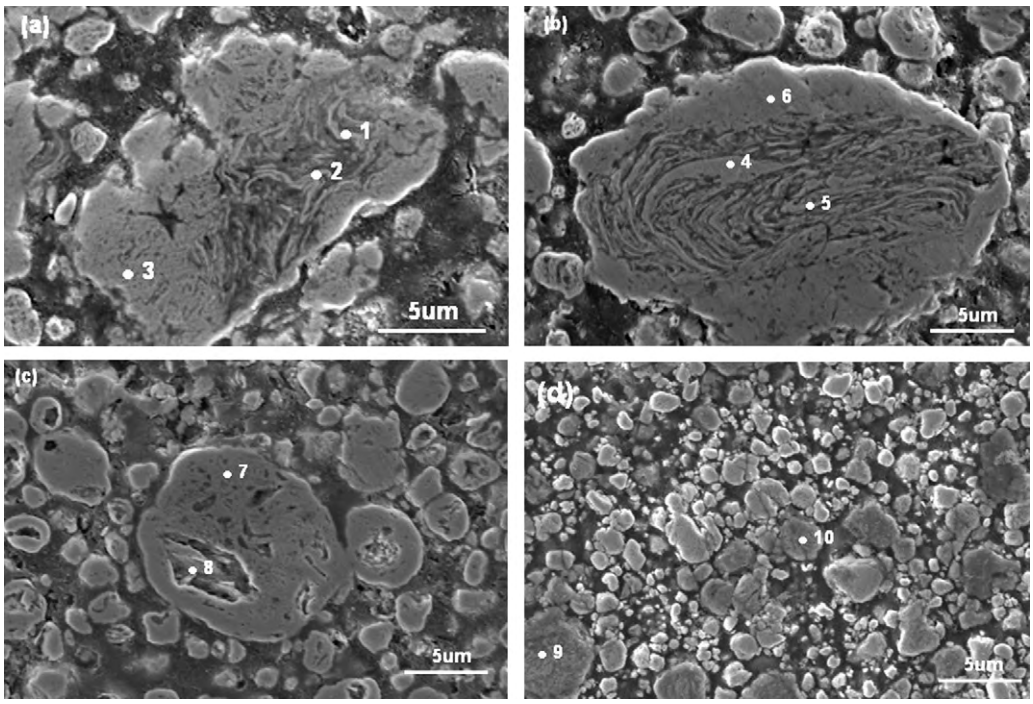

Fig. 3. SEM cross-sectional images of the Fe–40Al–5Cr powders milled for different times: (a) 5, (b) 15, (c) 35 and (d) 70 h.

and Fe–Cr(Al) phases of the milled Fe–40Al–5Cr powders. Compared with the 35 h milled powders, the 70 h milled Fe–40Al–5Cr powders are finer with an average particle size range from 125 to 200 nm (Fig. 2c). Only a halo appears in the SAED pattern, indicating that the 70 h milled powders are close to an amorphous structure (Fig. 2d). It was deduced that both the particle size and the ordering degree of the Fe–40Al–5Cr powders decreased with increasing the ball milling time. On the other hand, the SAED result in Fig. 2d seems not consistent with the XRD result, due to the appearance of the diffracting peaks of Fe(Al, Cr) in Fig. 1. Note that the intensity of the Fe(Al, Cr) diffraction peaks of the 70 h milled Fe–40Al–5Cr powders is very weak, therefore, the ordering degree of Fe(Al, Cr) should be actually in a rather low state, even near to an amorphous structure.

3.2. Alloying mechanism of the Fe–40Al–5Cr powders during mechanical alloying

The morphology of the 5 h milled Fe–40Al–5Cr powders is irregular with a wide particle size distribution. Some particles are larger than 30 μm, and the others are around 5 μm or smaller (Fig. 3a). There exist two different micro-zones across the cross-section of the large particle shown in Fig. 3a. In the center of the particle, the elongated laminae are present; however, around the elongated laminae, a continuous and dense shell forms with variable thickness. It is well known that the plastic deformation and cold-welding is the predominating process in the early stage of mechanical alloying of the plastic powder system, which promotes the formation of the elongated laminae composite structure. In these laminae, some are only composed of Fe and Al, in which the Cr content is close to zero (point #1 in Table 1). The others are the Fe–Cr powders having a limited Al content (point #2 in Table 1). Therefore, in the center of the particle, the Fe(Al) laminae and the Fe–Cr(Al) laminae are randomly distributed. The outside of the particle is more severely cold-welded due to high-energy impact of the milling balls, in which the Fe(Al) and Fe–Cr(Al) laminae roughly disappear, and a dense shell forms. In the shell, both Al and Cr compositions are rather high (point #3 in Table 1), indicating that the composition homogenization of Fe, Al and Cr preferentially occurs over there. The phenomenon of the co-existence of the Fe(Al) and Fe–Cr(Al) laminae in Fig. 2a are corresponding to the XRD result in Fig. 1, in which the separable XRD diffraction peaks of Fe(Al) and Fe–Cr(Al) were detected for the 5 h milled Fe–40Al–5Cr powders.

As shown in Fig. 3b, the particle size of the 15 h milled Fe–40Al–5Cr powders is still distributed widely, like that of the 5 h milled powders. However, the 15 h milled powders are more spherical. Two different micro-zones across the cross-sections of the 15 h milled powders still exist. There are the elongated Fe(Al)/Fe–Cr laminae in the center of the big particle, where the Cr/Al content is nil (points #4 and #5 in Table 1, respectively). The outside of the particle is denser, and has a ternary composition (point #6 in Table 1). As increasing the milling time, the average particle size of the milled powders decreases. The 35 h milled Fe–40Al–5Cr powders are mostly less than 5 μm with a narrow particle size distribution. The particles are dense and uniform without the laminae structure in the center (Fig. 3c). Note that there is a core in the center of a big particle, having a higher Cr content than elsewhere (points #7 and #8 in Table 1). The composition homogenization of the pow-

Table 1
EDX analyzing results of the different points marked in Fig. 3.

Elements	Composition/at%									
	#1	#2	#3	#4	#5	#6	#7	#8	#9	#10
Fe	67.0	74.08	59.7	74.3	77.76	58.97	57.99	62.26	49.93	52.1
Al	33.0	15.5	35.3	0	22.24	34.49	30.92	13.75	44.99	42.82
Cr	0	10.4	5.0	25.7	0	6.54	11.09	23.99	5.08	5.08

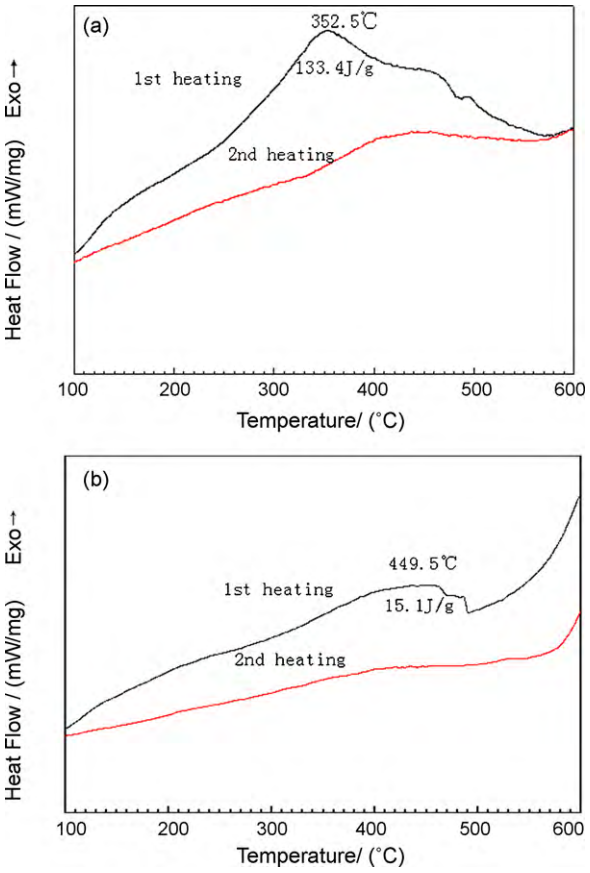

Fig. 4. DSC heating curves of the Fe–40Al–5Cr powders milled for different times: (a) 35 and (b) 70 h.

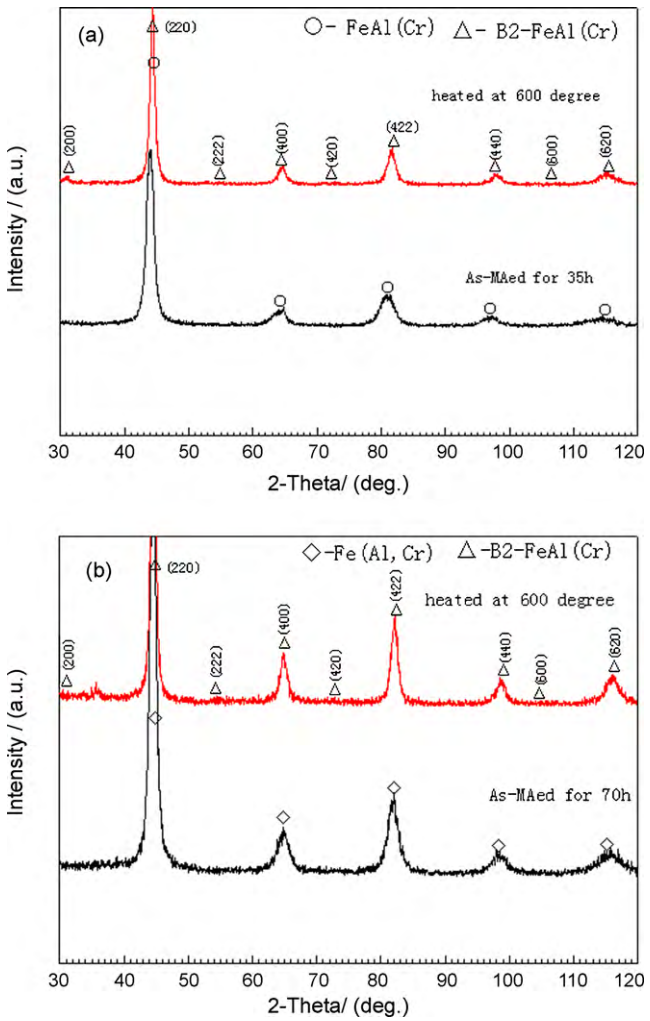

Fig. 5. XRD patterns of the (a) 35 and (b) 70 h milled Fe–40Al–5Cr powders after the DSC heating process, respectively.

ders has not accomplished yet at this time. Most of the 70 h milled Fe–40Al–5Cr powders is below 3 μm in diameter, meanwhile, the spheroidizing degree and the density of the particles are the highest (Fig. 3d). Furthermore, the composition of the 70 h milled powders was measured by EDX is 52.1 at%Fe, 42.8 at%Al and 5.1 at%Cr, almost equal to the nominal composition of the Fe–40Al–5Cr powders, indicating that the composition homogenization has nearly achieved after the powders milled for 70 h.

In summary, in the early stage of mechanical alloying (5–15 h), big agglomerated particles are formed through the plastic deformation and cold-welding of the Fe–40Al–5Cr powders. The elongated laminae of Fe(Al) and Fe–Cr(Al) are distributed in the center of the particles, while dense and continuous shells exist around them. Alloying at the outside of the particles is faster because of a heavy deformation and cold-welding over there. On prolonging the milling time from 15 to 35 h, fracture of big particles is predominated, accompanying with the composition homogenization of the Fe–40Al–5Cr powders. In the 35 h milled powders, the elongated laminae disappear, the composition of Fe, Al and Cr in the particles are more uniform. The 70 h milled Fe–40Al–5Cr powders are the finest and the most spherical than before. The powders are composed of Fe(Al, Cr), having a homogeneous composition, almost equal to the nominal composition of the Fe–40Al–5Cr powders.

3.3. Ordering transformation of the milled Fe–40Al–5Cr powders during heat treatment

The DSC curves of the Fe–40Al–5Cr powders milled for 35 and 70 h were shown in Fig. 4a and b, respectively. During heating from room temperature to 600 °C, both the 35 and 70 h milled Fe–40Al–5Cr powders suffer an exothermic transformation. And, the second DSC heating curves of them are always more flat than the first heating ones, which can be roughly taken as the baselines. As for the 35 h milled powders, there is a main exothermic peak at 352.5 °C in the first heating curve with a heat release of 133.4 J/g (Fig. 4a). Similarly, there is a main exothermic peak at 449.5 °C in the first DSC heating curve of the 70 h milled powders with a heat release of 15.1 J/g (Fig. 4b). Apparently, during the DSC heating, the structural transformation of the 35 h milled powders takes place at a lower temperature, but with a larger heat release, compared with that of the 70 h milled powders. The flat second DSC heating curves of these two powders may show that the ordering transformation of the powders has nearly finished in the first DSC heating process.

To clarify the structural transformation of the milled Fe–40Al–5Cr powders during the DSC heating process, the DSC heated powders were analyzed using XRD, and the results were shown in Fig. 5. After the DSC heating, all XRD diffraction peaks of the milled Fe–40Al–5Cr powders turn to be sharper with a higher intensity than those of the as-mechanical alloyed powders, which partially attributes to the structural evolutions of the milled Fe–40Al–5Cr powders during heating process, such as grain growth, release of internal stress and so on [16]. More importantly, as shown in Figs. 5a and b, the superlattice diffraction peaks of B2-FeAl(Cr) (2 0 0) and (2 2 2) appear in the XRD patterns of the heated Fe–40Al–5Cr powders. This means during the DSC heating, the ordering transformation from Fe(Al, Cr) to B2-FeAl(Cr)

has taken place. The intensity of the superlattice diffraction peaks of the 35 h milled powders is higher than those of the 70 h milled powders, indicating that the ordering transformation of the 35 h milled powders is more intensive in the DSC heating process.

Muñoz-Morris et al. [17] have reported that in the DSC curves of the milled Fe–40Al powders, the exothermic peak at 300–450 °C is related to the reaction between the unalloyed Fe and Al powders to form B2-FeAl. In the current study, the exothermic peaks in the DSC curves of the 35 and 70 h milled Fe–40Cr–5Cr powders are both in the range from 352.5 to 449.5 °C, which are situated in the temperature range of 300–450 °C [17]. The exothermic peaks in Fig. 4 refer to the reaction between the unalloyed Fe(Al) and Fe–Cr(Al) powders to form B2-FeAl(Cr). As mentioned in Sections 3.1 and 3.2, the alloying extent of the 35 h milled powders is unaccomplished, leaving the heterogeneous Fe(Al) and Fe–Cr(Al) powders in them. In the DSC heating process, the Fe(Al) and Fe–Cr(Al) powders react to form B2-FeAl(Cr) with a higher heat release (Fig. 4). On the contrary, alloying of the 70 h milled Fe–40Al–5Cr powders are nearly achieved to form the homogenous Fe(Al, Cr) powders. During DSC heating process, the lower heat release for the 70 h milled Fe–40Al–5Cr powders is reasonable. Moreover, the higher DSC peak temperature of the 70 h milled Fe–40Al–5Cr powders hints that Cr in Fe(Al, Cr) may inhibit the inter-diffusion of Fe, Al and Cr in Fe(Al, Cr), and hence, hinder the ordering transformation from Fe(Al, Cr) to B2-FeAl(Cr).

4. Conclusions

(1) Nanocrystalline Fe–40Al–5Cr powders were synthesized by mechanical alloying the Fe, Al elemental powders and the Fe–20Cr prealloyed powders. After milled for 70 h, the Fe–40Al–5Cr powders are the homogeneous Fe(Al,Cr) powders having a grain size of about 12.9 nm and a lattice strain of around 0.3%.

(2) In the early stage of milling the Fe–40Al–5Cr powders (5–15 h), the solid solutions of Fe(Al) and Fe–Cr(Al) are formed. The Al atoms dissolve preferentially into Fe(Al) than into Fe–Cr(Al). After the Fe–40Al–5Cr powders milled for 35 h, the Al content in Fe(Al) was calculated to be 22.4 at%, the highest Al content in Fe(Al) throughout this mechanical alloying process. On prolonging the milling time from 15 to 70 h, the mutual diffusion between Al in Fe(Al) and Cr in Fe–Cr(Al) leads to the composition homogenization of the milled powders. After the Fe–40Al–5Cr powders milled for 70 h, a homogeneous Fe(Al, Cr) solid solution is formed having a rather low lattice ordering degree.

(3) During mechanical alloying, the agglomerates are firstly formed through the plastic deformation and cold-welding of the Fe–40Al–5Cr powders. The elongated Fe(Al) and Fe–Cr(Al) laminae are randomly distributed in the center of the particles. As prolonging the milling time, the agglomerates are broken into small ones, the elongated laminae in them gradually disappear, and the uniform and dense particles form. The 70 h milled powders are ultrafine and spherical with a homogenous composition equal to the nominal composition of the Fe–40Al–5Cr powders.

(4) During DSC heating the milled Fe–40Al–5Cr powders from room temperature to 600 °C, the ordering transformation from Fe(Al, Cr) to B2-FeAl(Cr) occurs. The higher DSC peak temperature of the 70 h milled powders hints that Cr in Fe(Al, Cr) may hinder the ordering transformation.

Acknowledgment

This study is financially supported by Natural Science Foundation of Anhui Province, China (090414193).

References

[1] S.E. Haghighi, K. Janghorban, S. Izadi, J. Alloys Compd. 495 (2010) 260–264.
[2] I.Y. Ko, S.H. Jo, J.M. Doh, J.K. Yoon, I.J. Shon, J. Alloys Compd. 496 (2010) L1–L3.
[3] L.D. Angelo, L.D. Onofrio, G. Gonzalez, J. Alloys Compd. 483 (2009) 154–158.
[4] S. Izadi, K. Janghorban, G.H. Akbari, M. Ghafari, E. Salahinejad, J. Alloys Compd. 493 (2010) 645–648.
[5] C.G. McKamey, J.A. Horton, C.T. Liu, J. Mater. Res. 4 (1989) 1156–1163.
[6] N.S. Stoloff, Mater. Sci. Eng. 258A (1998) 1–14.
[7] W.M. Tang, H.J. Tang, Z.X. Zheng, Y.C. Wu, J.L. Dong, J. Hefei Univ. Technol. 8 (2005) 129–134 (in Chinese).
[8] D.G. Morris, A.M. Muñoz-Morris, J. Chao, Intermetallics 12 (2004) 821–826.
[9] R.A. Rodriguez-Diaz, M. Suarez, J. Juarez-Islas, J. Appl. Res. Technol. 7 (2009) 233–244.
[10] W.M. Tang, Z.X. Zheng, H.J. Tang, R. Ren, Y.C. Wu, Intermetallics 15 (2007) 1020–1026.
[11] B. Huang, R.L. Perez, E.J. Lavernia, Mater. Sci. Eng. 225A (1998) 124–132.
[12] C. Suryararayana, Prog. Mater. Sci. 46 (2001) 1–184.
[13] A. Heesemann, E. Schmidtke, F. Faupel, Scr. Mater. 40 (1999) 517–522.
[14] M. Eggersmann, H. Mehrer, Philos. Mag. 80A (2000) 1219–1244.
[15] G.K. Williamson, W.H. Hall, Acta Metall. (1953) 23–31.
[16] B.S. Murty, S. Ranganathan, Int. Mater. Rev. 43 (1998) 101–141.
[17] M. Muñoz-Morris, A. Dodge, D.G. Morris, Nanostruct. Mater. 11 (1999) 873–885.